To be presented at 17 Conf. on Boundary Element Methods.
Madison, Wisconsin, July 17-19, 1995



SAND95-1196C
CONF-9507125--2

# A Numerical Model for 2-D Sloshing of Pseudo-Viscous Liquids in Horizontally Accelerated Rectangular Containers

Vicente J. Romero (Sandia National Laboratories) and
Marc S. Ingber (University of New Mexico Dept. of Mech. Engr.)
Albuquerque, New Mexico, USA



## Abstract

A numerical model for simulating the transient nonlinear behavior of 2-D viscous sloshing flows in rectangular containers subjected to arbitrary horizontal accelerations is presented. The potential-flow formulation uses Rayleigh damping to approximate the effects of viscosity, and Lagrangian node movement is used to accommodate violent sloshing motions. A boundary element approach is used to efficiently handle the time-changing fluid geometry. Additionally, a corrected equation is presented for the constraint condition relating normal and tangential derivatives of the velocity potential where the fluid free surface meets the rigid container wall. The numerical model appears to be more accurate than previous sloshing models, as determined by comparison against exact analytic solutions and results of previously published models.

## I. Introduction and Background

The prediction of the sloshing behavior of liquids in externally excited containers finds application in robotic movement of containers, vehicle dynamics and control, earthquake engineering, and many other important pursuits. Multiple nonlinear constraints at the fluid free surface, special behavior at "contact points" where the free surface meets rigid boundaries, and the difficulties associated with a fluid domain that evolves in time in a manner not known *a priori* (the evolution of the fluid domain is coupled into the problem and must be solved for), make the problem an interesting and challenging one.

It is frequently the case that sloshing can be successfully modelled as potential flow, in which an inviscid and incompressible liquid experiences irrotational motion. Under these assumptions, Laplace's equation governs the flow. We note that Laplace's equation is a linear elliptic partial differential equation (PDE). Nonlinearity and time-dependence enter into the initial



This work was supported by the United States Department of Energy under Contract DE-AC04-94AL85000.

## DISCLAIMER

boundary value problem through two conditions at the free surface that must be satisfied simultaneously. The nonlinear "dynamic condition" reflects the interplay of forces and momenta at the free surface, and the so-called "kinematic condition" provides the prescription for moving the mathematical representation of the free surface in accordance with physical considerations of the fluid motion. In the discrete problem, the kinematic condition generally yields nonlinear equations governing $x$ and $y$ position of free-surface nodes.

In the linearized problem (see e.g. references [1] and [2]), the nonlinear terms in the dynamic condition are dropped and displacements of the free surface from the equilibrium (resting) level are assumed small enough that both the dynamic and kinematic conditions can be evaluated at the rest level. The linearized time-periodic small-amplitude sloshing problem yields an eigenproblem for sloshing modes and frequencies that has been solved analytically or numerically for various fluid depths and container geometries (see the books [1]-[3] and the reviews [4]-[7]). Numerical solutions to non time-periodic ("unsteady") linearized and quasi-linear sloshing problems have been attempted with finite element methods (see e.g. [8]-[11]), as well as with boundary element techniques ([12], [13]). Boundary element techniques offer a substantial advantage over domain-based methods in that only the boundary of the fluid domain must be discretized as opposed to the entire domain. Thus, boundary element approaches are especially suited for free-surface flows, which involve a fluid domain that changes over time.

A boundary element formulation for the fully nonlinear (large amplitude) sloshing problem has been published in [14] for a stationary rectangular container. Faltinsen's model [15] includes Rayleigh damping to dissipate fluid motion over time (as occurs in real liquids) but is limited to relatively small horizontal container displacements. Nakayama & Washizu [13] employed a transformation to coordinates moving with the container so that arbitrary horizontal motions could be applied, but the transformation linearized the dynamic equation, resulting in a "quasi-linear" formulation. Pauwelussen [16] solved the full nonlinear problem without horizontal motion restrictions, but did not include damping and did not explicitly account for constraints where the fluid free surface meets the walls of the container.

In this paper we present a numerical model for fully nonlinear unsteady sloshing of a Rayleigh-damped fluid in a rectangular container subjected to time-varying horizontal accelerations. Surface tension is neglected. We use a boundary element approach in solving Laplace's equation to efficiently handle the changing fluid geometry. The initial boundary value problem is formulated so that other time-integration packages can be easily substituted. A corrected constraint equation is presented for the contact-point condition where the fluid free surface meets a solid body. Finally, we apply the model to a standard benchmark problem and compare our results to some previously published results.

## II. Model Problem

In the pursuing development, it is helpful to be apprised of the application in mind so that we may quickly arrive at specific forms of the applicable equations and boundary conditions. The model problem of a rectangular container subjected to sinusoidal horizontal oscillation (see Figure 1) has been tried previously by several other researchers, e.g. [13], [15], [16].

Initially the container of width $w$ is at rest, holding a quiescent body of liquid of depth $d$ (relative to the bottom of the container). The container displacement $\delta_c$ and velocity $v_c$ from its initial position are given by

$$\delta_c = A\sin\omega t \tag{1}$$

and

$$v_c = A\omega\cos\omega t \tag{2}$$

where $\omega$ is the angular frequency of the oscillation. In terms of the period $T_p$ of the oscillation, $\omega$ is given by

$$\omega = 2\pi/T_p \tag{3}$$

The container is assumed to extend into and out of the page far enough that end-effects are negligible and a two-dimensional (2-D) treatment applies.

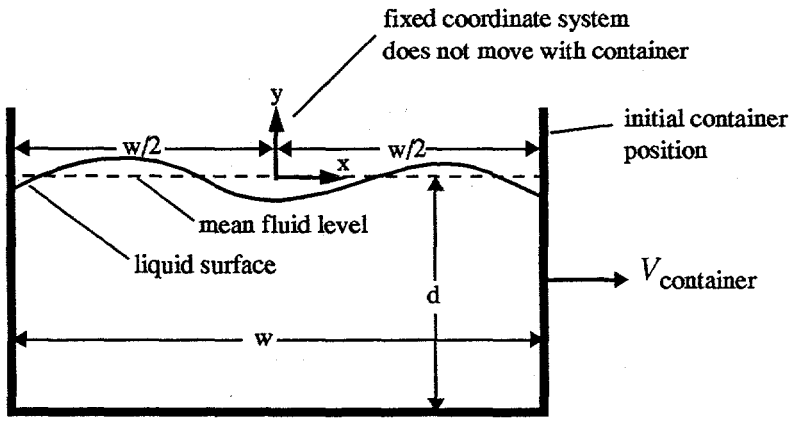


**Figure 1:** Model problem: a horizontally oscillating container holding fluid

## III. Governing Equations

We work from the fixed $x$-$y$ coordinate system depicted in Figure 2, with unit vectors in the $x$ and $y$ directions being $\hat{i}$ and $\hat{j}$, respectively. To model the motion of the fluid, momentum conservation must be applied. Assuming the fluid to be irrotational, *i.e.* the curl of the velocity is everywhere zero ( $\nabla \times \vec{v}_{fluid} = 0$ ), a velocity potential $\phi(x, y, t)$ governs the flow field such that it's gradient represents the fluid velocity at any point:

$$\vec{v}_{fluid} = \nabla\phi \tag{4}$$

Assuming incompressibility, conservation of mass requires that the divergence of the velocity be zero everywhere within the fluid. This translates to the requirement that $\phi$ satisfy Laplace's equation in the domain:

$$\nabla \bullet \vec{v}_{fluid} = 0 \quad \Rightarrow \quad \nabla^2\phi = 0 \quad \text{in fluid domain} \tag{5}$$

Under the additional assumption of negligible viscous effects (which completes the set of assumptions characterizing potential flow), the time-consistency of the problem is established by Kelvin's theorem (see [2]), which states that an inviscid and initially irrotational flow will always remain irrotational, and therefore that Laplace's equation will apply throughout time. Though a real fluid might eventually depart from irrotationality, these assumptions seem in practice to hold reasonably well throughout time for problems where water is the fluid and the container motion is not exceedingly violent.

From the consideration that the fluid boundary must conform to rigid surfaces but the fluid may slip tangentially along the surface for inviscid flow, boundary movement on a fluid/solid interface is constrained according to

$$\hat{n} \bullet \vec{v}_{fluid} = \hat{n} \bullet \vec{v}_{wall} \quad \text{at solid boundaries} \tag{6}$$

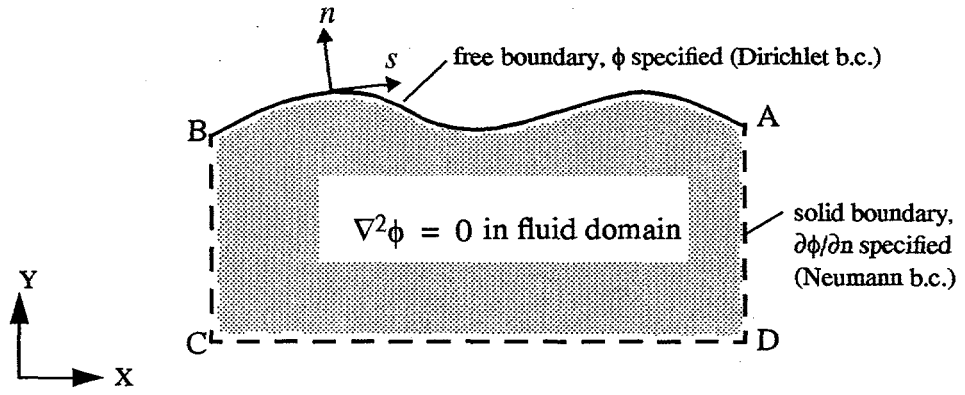


**Figure 2:** Laplace problem associated with the example sloshing problem

where $\vec{v}_{wall}$ is the local velocity of the rigid surface and $\hat{n}$ is a unit vector locally normal to the domain boundary and pointing away from the interior of the domain as shown in Figure 2. Using equation (4) in (6) yields a Neumann boundary condition at solid/fluid interfaces for the Laplace problem

$$\frac{\partial \phi}{\partial n} = \hat{n} \bullet \vec{v}_{wall} \qquad \text{at solid boundaries} \tag{7}$$

We will address the movement of nodes on solid/fluid interfaces later.

At the free surface the kinematic condition reflects the fact that for points on the mathematical boundary to track the fluid surface their velocities relative to the fluid at the surface must be "either wholly tangential or zero" (Lamb, [1]). If the relative velocity is zero, then the point moves as though it were a fluid particle at the free surface. Adopting this convention to move our computational nodes on the free surface, we have

$$\vec{v}_{node} = \vec{v}_{fluid} = \nabla \phi \qquad \text{at the free surface} \tag{8}$$

Though other conventions exist that satisfy the kinematic condition (see e.g. [17]), "Lagrangian" movement has unique properties that would appear to make it well suited for simulation of high-amplitude sloshing flows. Lagrangian node movement has been very successfully used to model highly nonlinear, impulsive, and violent flows such as those generated by piston wavemakers or oscillating floating bodies, with waves eventually crashing (overturning) or impacting tilted or vertical walls (see e.g. [18]-[22]).

Considering that $\vec{v}_{node}$ is the time derivative of nodal position $\vec{r}_{node}$ (= $x_{node}\hat{i} + y_{node}\hat{j}$), we have

$$\vec{v}_{node} = \frac{d}{dt}(\vec{r}_{node}) = \frac{d}{dt}(x_{node})\,\hat{i} + \frac{d}{dt}(y_{node})\,\hat{j} = \dot{x}_{node}\hat{i} + \dot{y}_{node}\hat{j} \tag{9}$$

Dotting the vector equation (8) with $\hat{i}$, then $\hat{j}$, and using the notation established in eqn. (9) yields the following two ordinary differential equations (ODEs) for Cartesian position of free-surface nodes.

$$\dot{x}_{node} = (\hat{i} \bullet \hat{n})\frac{\partial \phi}{\partial n} + (\hat{i} \bullet \hat{s})\frac{\partial \phi}{\partial s} \qquad \text{at the free surface} \tag{10}$$

$$\dot{y}_{node} = (\hat{j} \bullet \hat{n})\frac{\partial \phi}{\partial n} + (\hat{j} \bullet \hat{s})\frac{\partial \phi}{\partial s} \qquad \text{at the free surface} \tag{11}$$

In the above we have assumed a form of $\nabla \phi$ in terms of its normal ($n$) and tangential ($s$) components,

$$\nabla \phi = \frac{\partial \phi}{\partial n}\hat{n} + \frac{\partial \phi}{\partial s}\hat{s}. \tag{12}$$

We use the form (12) because, as will be shown later, our integral-equation method for solving Laplace's equation yields $\partial\phi/\partial n$ directly, and $\partial\phi/\partial s$ can be easily found by numerical differentiation.

A Dirichlet boundary condition for the Laplace problem is obtained at the free surface via the unsteady Bernoulli equation, which applies within and on the boundary of the fluid. A derivation of this equation, which proceeds from consideration of momentum conservation along a flow streamline, may be found in [2], where the additional assumption beyond those already mentioned of conservative body forces (here due to gravity) is invoked. Reference [15] indicates how a simplifying mechanism to account for the major effects of viscosity may be included in the momentum equation according to a device originally proposed by Lord Rayleigh. Such "Rayleigh damping" acts to dissipate momentum by opposing fluid motion with a force proportional to the local gradient of fluid velocity. The constant of proportionality or "viscosity coefficient" $\mu$ changes with the flow regime and is best set by comparison with experiments or computer analyses solving the full Navier-Stokes fluid-flow equations (see e.g. [23]).

Applied at the free surface, the damping-modified unsteady Bernoulli equation becomes

$$\frac{\partial\phi}{\partial t} = -\left[\frac{V^2}{2} + gy + \mu\phi\right] \qquad \text{at the free surface} \qquad (13)$$

where $y$ is the vertical coordinate (height of the free surface relative to the $x$ axis), $g$ is the magnitude of gravitational acceleration, $V$ is the fluid speed (magnitude of the local velocity vector $\vec{v}_{fluid}$), and atmospheric pressure has been assumed constant all along the free surface.

When Bernoulli's equation is applied at the free surface it is known as the "dynamic condition" in free-surface potential-flow nomenclature. We employ it to update the velocity potential $\phi$ on the free surface as the simulation progresses in time. This provides a Dirichlet boundary condition at the free surface that is used in solving Laplace's equation.

We note that Equation (13) pertains to the partial or "Eulerian" time derivative of the velocity potential $\phi(x, y, t)$, taken while holding $x$-$y$ position fixed. However, we must use the total time-derivative (see e.g. [24]) in updating $\phi$ on the **moving** free surface. For a node moving as a fluid particle the total time-rate-of-change of its velocity potential is given by (*cf* [25])

$$\dot{\phi}_{node} = \frac{D\phi}{Dt} = \frac{1}{2}\left[\left(\frac{\partial\phi}{\partial n}\right)^2 + \left(\frac{\partial\phi}{\partial s}\right)^2\right] - gy - \mu\phi \qquad \text{at the free surface} \qquad (14)$$

## IV. Outline of Numerical Solution Procedures

### *Method-of-Lines Approach to Initial Boundary Value Problem*

To recap, we may fully characterize the sloshing flow over the time span of interest by resolving the time-dependent velocity field within the domain. This translates via eqn. (4) to the requirement that we determine the time evolution of the velocity potential $\phi$ over the time-changing domain. To accomplish this we must time-march a set of 3N coupled nonlinear ordinary differential equations (eqns. (10), (11), and (14) are written at each of the N free-surface nodes) while simultaneously requiring $\phi$ to satisfy Laplace's equation over the domain. We may conceptualize the complete ODE set in standard ODE matrix notation:

$$\{\dot{w}_k\} = \left[A(\{w_k\}, t)\right]\{w_k\} \tag{15}$$

where it has been emphasized that the coefficient matrix $[A]$ is a function of $\{w_k\}$ for a set of nonlinear ODEs, and has an explicit dependence upon time if prescribed changes in geometry and Neumann conditions at solid boundaries occur.

Standard explicit time-marching methods predicated upon the form (15) (see e.g. [26]) can be applied to advance the set of ODEs in time, assuming that the quantities on the right-hand-sides (RHSs) of equations (10), (11), and (14) are known at the beginning of each time step. To determine the spatial derivatives on the RHSs of these equations, we must solve the elliptic boundary-value problem presented generically in Figure 2. The Neumann b.c.s on the nonfree portions of the boundary are known from eqn. (7) and the time-specified container motion. From initial conditions of specified geometry and specified velocity potential (*i.e.* Dirichlet boundary condition) on the free surface we have a closed Laplace problem to start. It's solution, and subsequent spatial differencing, yields the required derivatives $\partial\phi/\partial n$ and $\partial\phi/\partial s$. All information necessary for advancing the solution by one time-step is now known. Each time-step updates the locations of free-surface nodes and the Dirichlet boundary condition (velocity potential) at the free surface. This, along with the time-prescribed information in the problem, sets up a new Laplace problem to be solved in preparation for taking the next time step. Thus, the computation progresses and the solution unfolds in time.

A variable-step 4th/5th order Runge-Kutta integrator (DERK45 [27] from the SLATEC library [28]) has been chosen for the present work. It has been found to advance the nonstiff set of ODEs with a good balance of accuracy, economy, and stability. However, other integrators have also been used with good success. The modular method-of-lines formulation we've outlined allows quick substitution/evaluation of different integration packages, whereas less standardized approaches such as the 'incremental' time-marching method in [13], the Taylor-Series method of Dold & Peregrine [29], and the implicit technique of Liu & Liggett (see e.g. [17]), do not enjoy this benefit.

## Boundary Element Solution Method for Laplace's Equation

Although domain methods have been employed in solving free-surface potential-flow problems there is tangible evidence that boundary integral techniques offer superior performance for this type of problem ([30]-[32]). The direct boundary element method (DBEM, [33]) is particularly accurate and efficient at solving Laplace's equation, and is extensible to 3-D whereas some other integral-equation techniques (see [34], [35] for reviews) are not.

For our 2-D example problem we use the DBEM to solve the following Fredholm boundary integral equation (BIE):

$$\alpha(\underset{\sim}{p})\,\phi(\underset{\sim}{p}) = \int_{\Gamma}\left[\phi(\underset{\sim}{\xi})\frac{\partial}{\partial n}\ln r(\underset{\sim}{\xi},\underset{\sim}{p}) - \ln r(\underset{\sim}{\xi},\underset{\sim}{p})\frac{\partial\phi}{\partial n}(\underset{\sim}{\xi})\right]d\Gamma(\underset{\sim}{\xi}) \qquad (16)$$

where $\phi(\underset{\sim}{p})$ is the velocity potential at a particular point $p$ on the boundary, $\alpha(\underset{\sim}{p})$ is the internal angle of the boundary contour there (see Figure 3), $\ln r$ is the value at $\underset{\sim}{\xi}$ of $2\pi$ times the 2-D free-space Green's function centered at $\underset{\sim}{p}$ and $r = |\underset{\sim}{\xi} - \underset{\sim}{p}|$. The operator $\partial(\ )/\partial n$ finds the rate of change of the operated quantity in the direction normal to the boundary and pointing away from the interior of the domain.

Using the principle of collocation, Equation (16) is written at all nodes on the domain boundary. Using standard discretization techniques [33], these BIE are represented in discrete form and assembled into a set of globally coupled linear algebraic equations that can be solved by Gaussian elimination. The formulation yields computed velocity potentials $\phi_i$ at nodes where a Neumann boundary condition is specified, and yields computed normal derivatives $(\partial\phi/\partial n)_i$ at nodes where a Dirichlet condition is specified.

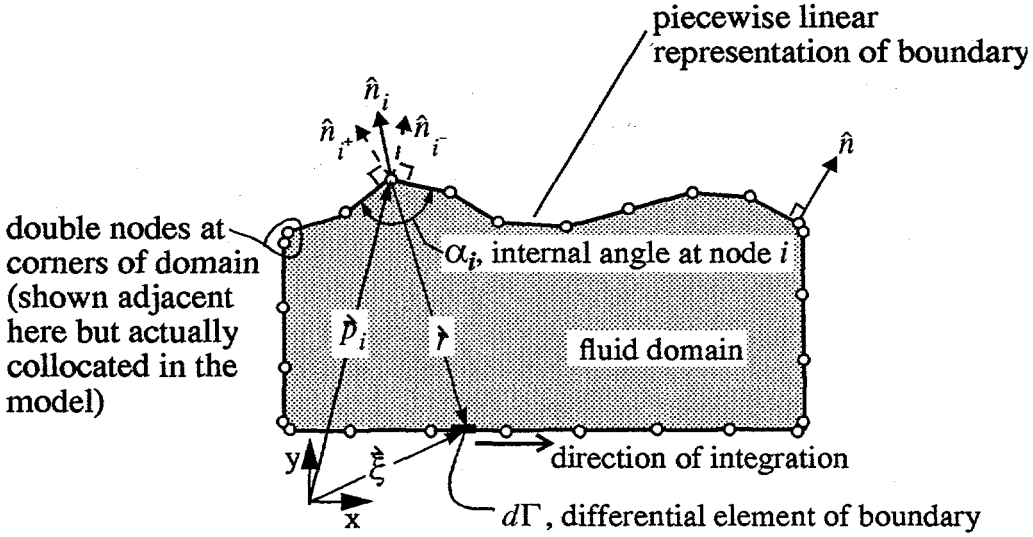


**Figure 3:** Boundary element model of fluid domain

The present formulation uses a piecewise linear approximation to the domain boundary. Linear isoparametric boundary elements are employed which allow exact analytic integrations (see e.g. [36]) of Green's function and its normal derivative over the elements. Other types of boundary elements and integration methods have been used in free-surface problems with good success (e.g. [15], [20], [37]-[40]). However, formulations using higher-order elements are more complex and also may suffer from deleterious effects when the free-surface nodes in the physical space drift away from their assumed parametric positions in the shape functions (see [41]).

As Figure 3 shows, the nodes on the ends of the piecewise-linear approximation to the free surface have unambiguous normal directions, but the other free-surface nodes do not. To resolve this we first define a boundary tangency angle $\beta$ in Figure 4. The tangency angles of the two boundary elements adjoined at a node are averaged, yielding the value $\beta_i$. The nodal tangent $\hat{s}_i$ is then said to have this average tangency angle. The nodal normals $\hat{n}_i$ are rotated 90 degrees counter-clockwise from the nodal tangents.

Instead of using geometry to calculate the internal angle of the domain at the free-surface node points (the $\alpha_i$ in Figure 3), we use eqn. (16) and the well-known device of assuming a constant potential over the domain (see [33]) to calculate $\alpha_i$ in terms of the off-diagonal elements in the coefficient matrix of the assembled BIEs. This self-consistent method of determining $\alpha_i$ has been shown to lower the condition matrix of the BIE system significantly [19].

A double-node technique is used to address the very large differences in the normal directions of the boundary elements adjoined at the four vertices of the domain, denoted A, B, C, and D in Figure 2. This allows two distinct Neumann conditions, one in each normal direction as the corner is approached from one side then the other, to coexist at the corner. Operationally, two computational nodes are placed at each vertex, one associated with each of the adjoining

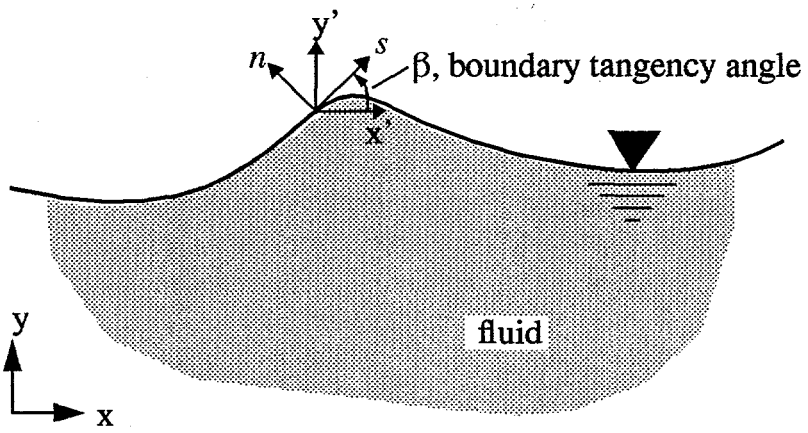


**Figure 4:** Boundary tangency angle $\beta$

boundary segments, and BIEs are written at the nodes and assembled into the set of discretized equations according as the boundary condition prescribed on the adjoining segment is Neumann or Dirichlet. (This approach works very well and is simpler to program than "splitting" the potential [16] or inserting a constraint equation for continuity of potential at the collocated nodes as suggested in [20], [22], [40], and [42].)

### *Numerical Determination of Tangential Derivatives on the Free Surface*

The normal and tangential derivatives of $\phi$ are needed for time-integrating the ODEs (10), (11), and (14). Although the solution of the BIEs directly yields $(\partial\phi/\partial n)_i$ at the free-surface nodes, we must determine $(\partial\phi/\partial s)_i$ separately. Although a more elegant method (the tangent-derivative BEM [43]) exists to determine $\partial\phi/\partial s$ at the free surface, numerical differencing is used in the present model for economy and simplicity. Following Liu & Liggett [44], a central difference approximation for $\partial\phi/\partial s$ that accounts for the (in general) different lengths of adjacent free-surface elements is used.

### *Implementation of the Constraint at Contact Points*

At the "contact points" A and B in Figure 2 where the free surface meets a solid boundary, a physically imposed constraint on the fluid velocity $\nabla\phi$ exists. The velocity of the container wall determines $\partial\phi/\partial x$ at the contact point via equation (7). Also, the solution to the BIEs yields $\partial\phi/\partial n$ on the fluid surface at the contact point. The value of $\partial\phi/\partial s$ is thus constrained such that dotting eqn. (12) by the direction vector $\hat{i}$ must equal the physically imposed value $\partial\phi/\partial x$. The proper algebraic manipulations lead to the result

$$\frac{\partial\phi}{\partial s} = \frac{v_c}{\cos\beta} + \tan\beta\,\frac{\partial\phi}{\partial n} \qquad \text{at contact points} \tag{17}$$

where $\beta$ is the angle between $\hat{i}$ and the tangent vector $\hat{s}$ at the fluid boundary (see Figure 4) and $v_c$ is the speed of the container wall as defined in eqn. (2).

Since the horizontal velocity at the contact point is known *a priori*, eqn. (10) does not have to be written for the free-surface node there, but the velocity potential and height of the fluid surface at the wall do depend upon a compatible value of $\partial\phi/\partial s$ in eqns. (11) and (14). We comment that the constraint (17) must be explicitly imposed on free-surface nodes at contact points when Lagrangian node movement is used. Apparently, only the formulation of Grilli and coworkers (see e.g. [40]) among the many works possessing similar circumstances (e.g. [16], [20], [22]) explicitly recognizes the compatability condition. However, eqn. (17), valid at both the left wall and the right wall of the container, differs from the result published in [40], which can be shown to be equivalent to (17) at the left wall but not at the right wall. Because nodes were not located at the contact points in Faultinsen's formulation [15], this constraint does not apply even though he used Lagrangian node movement. However, his model allows only very small horizontal container displacements. The formulation of Medina et. al. [14] pre-constrains node movement to be

exclusively in the vertical direction, and therefore implicitly respects the condition (17). However, the model is limited to the free sloshing of fluids in stationary containers. The method of Nakayama & Washizu [13] also uses constrained vertical node motion and therefore respects (17), but the transformation used to account for horizontal container movement does not contain all of the necessary terms for nonlinear free-surface motion. Finally, we note that equation (17) is only valid for vertical walls, but can be generalized to arbitrary wall angles from the same principles applied above.

*Miscellaneous*

It is appropriate here to mention that, as the solution progresses in time, the computational nodes between the free-surface contact point and the bottom of the domain are moved to maintain equal node spacing along the container walls.

A second special characteristic exists at contact points. Impulsive wall motions ($v_c$ discontinuous in time) will generate a mathematical singularity at the contact point [45]. Though more exotic elements and integration techniques exist to resolve such singularities (see e.g. [40]), we implement no special measures here. The numerical procedures used have proven adequate for the container motions examined in the next section, even with impulsive starts from rest.

Finally, it is worth mentioning that where "static" geometrical relations exist, boundary element contributions to the coefficients in the assembled BIE matrix do not have to be recomputed at each new timestep (see [33] pp. 124). This can lower total computation time significantly.

## V. Model Validation

The numerical model described above has been applied to the model problem defined in section II and the results are here compared to analytical and numerical results published in the literature.

It appears that the only previously published fully nonlinear computer model that accounts for all of the physics that the current model does is Faltinsen's [15]. However, Faltinsen's model and the current model are quite different numerically. Briefly, his model employs a fixed-step "central difference" time-marching method with constant boundary elements in an indirect boundary element formulation for solving Laplace's equation. Due to constraints on node movement the formulation breaks down when the absolute value of the free-surface tangency angle $\beta$ approaches large angles, like when large and violent free-surface motions are involved. Additionally, the container can only be moved relatively small horizontal distances about the starting position. Nevertheless, comparisons can be made within these limits.

The governing parameters for the validation problem are (refer to Figure 1 and section II): $w$ = 1 meter [m], $d$ = 0.5 m, $A$ = 0.025m, $T_p$ = 1.3 seconds [s], $g$ = 9.8 m/s$^2$, and $\mu = 0.05\mu_{crit}$. From [15] an estimate of the critical damping coefficient $\mu_{crit}$ is given by

$$\mu_{crit} = 2\sqrt{\frac{g\pi}{w}\tanh\left(\frac{d\pi}{w}\right)} \tag{18}$$

In the current model the boundary of the domain is divided into: 60 elements on the free surface, 30 elements on the bottom boundary, and 20 on either side. For the example problem this is probably more than sufficient to capture the local details of the fluid motion. (No attempt was made to duplicate the number of elements used in [15] in an effort to verify the current model by exact duplication of the published results because of the confounding effects of other algorithmic differences.) The nodes on the side and bottom boundaries are always equally spaced, even though the lengths of the side elements change as the fluid rides up and down the container walls. The lengths of the free-surface elements are not constrained in any way, but Lagrangian node movement tends to concentrate nodes in highly curved regions of the free surface wherever jets of liquid are formed [25]. This is in some ways desirable because of the natural increase in resolution at precisely the locations on the free surface where the curvature is large. However, when nodes are too close together, special numerical procedures may be required, depending upon the type of elements used and method of integration, to accurately solve the BIEs (see e.g. [40]). Additionally, the clustering of nodes may decrease the stability of the system, requiring smaller time steps to be taken or periodic regridding of the free surface. None of these special measures have been implemented in the current model.

Figure 5 shows the present model's prediction of fluid response as measured by deviation in surface height from the mean fluid level. Free-surface dispacement at a distance 0.05m from the left wall of the container (*i.e.* the

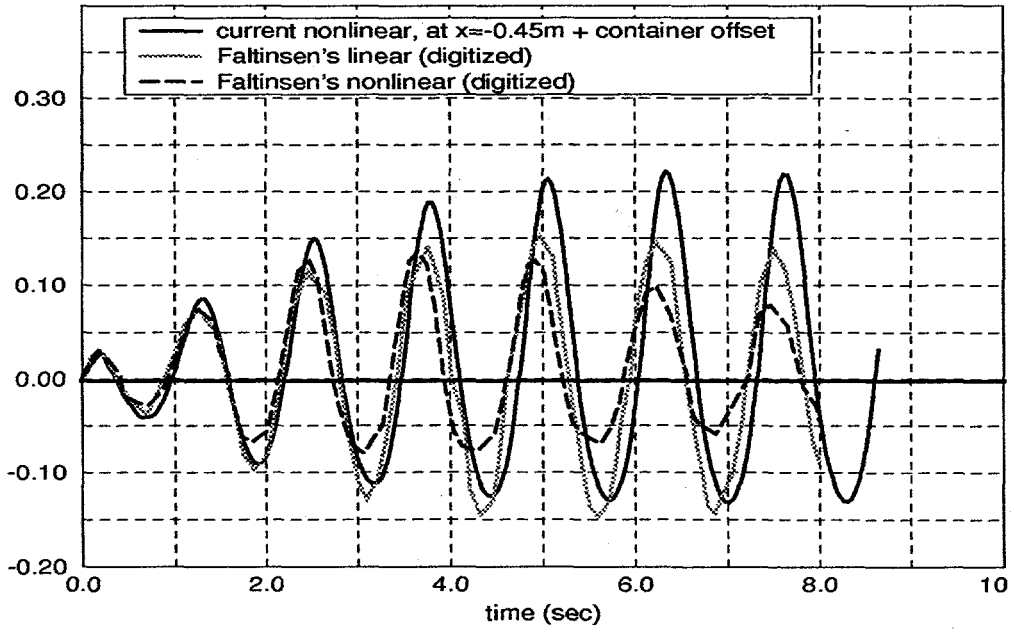


**Figure 5:** Free-surface displacement from rest level at a distance 0.05 m from left side of container. Container oscillation period = $T_p$ = 1.3 sec.

absolute location of the measurement point changes in time following the motion of the container) are plotted vs. time. Nonlinear and linear predictions digitized from [15] are also shown for comparison. The nonlinear solutions from the present model are quite different from Faltinsen's solution, and both nonlinear solutions are notably different from the linear solution, which probably does not apply very well for this very nonlinear example (note that the amplitudes of up to 22 cm are of the same order of magnitude as both the depth and the width of the domain). Though the amplitudes of the three solutions are considerably different, the phases all agree reasonably well. The nonlinear results produced by both Faltinsen's and the current model exhibit the characteristic trait of crests with substantially greater amplitude than troughs. This physically observed characteristic of nonlinear waves is not predicted by linear models. The nonlinear model of Faltinsen, however, predicts substantially lower crests than linear theory predicts. This is qualitative contrary to observed trends for nonlinear vs. linear waves, and thus provides an indication that the current model is probably more accurate than Faultinsen's.

Further evidence that the current model is more accurate than Faltinsen's is shown in Figure 6, which plots the predicted responses when the simulation is rerun with an oscillation period of $T_p$ = 1.6 seconds. The response is much less regular, presumably because the oscillation frequency is further from the predicted linear resonance frequency of 1.18 seconds (see [15]). For this much more linear problem (maximum amplitudes of about 7 cm), the present model

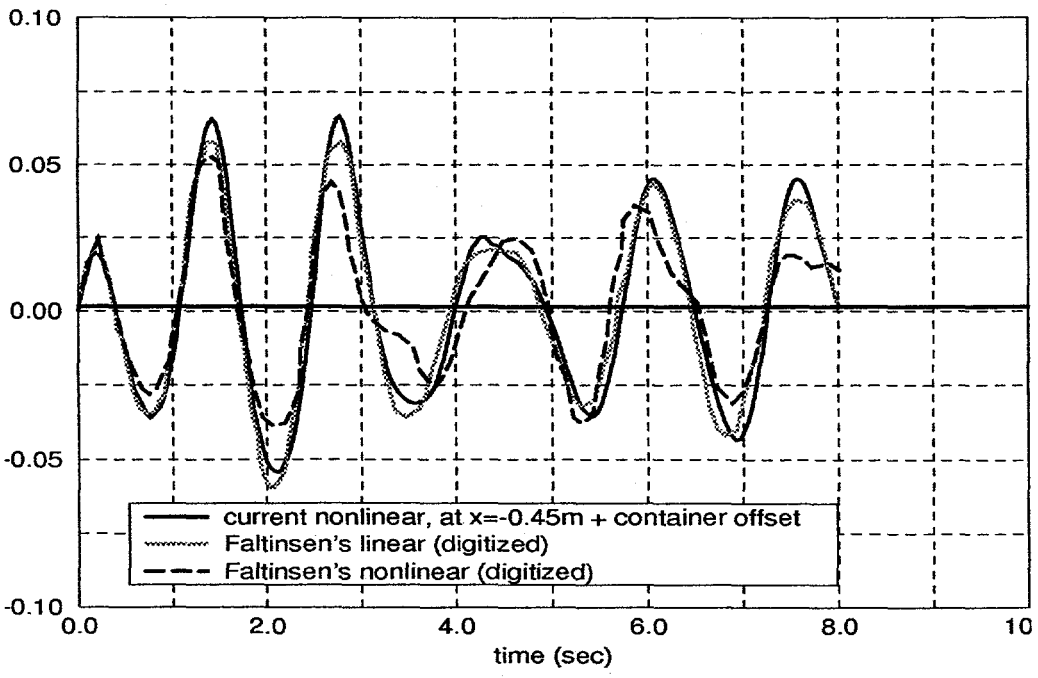


**Figure 6:** Free-surface displacement from rest level at a distance 0.05 m from left side of container. Container oscillation period = $T_p$ = 1.6 sec.

much more closely conforms to the linear predictions than does the nonlinear model of Faltinsen. We can expect that as the behavior becomes less and less nonlinear, the nonlinear solution should converge to the linear solution. The present model appears to possess this property much more than Faltinsen's.

For an oscillation period of $T_p$ = 1.2 seconds, Figure 7 shows the shape of the free surface when the container approaches its center of oscillatory motion at succeeding multiples of the oscillation period. A period of 1.2 seconds was determined by numerical experiment to excite the fluid motion in a most resonance-like condition (cause fastest amplitude growth). The calculation had to be suspended at $t$ = 4.4 seconds because of an instability that erupted shortly thereafter. At periods of 1.18 seconds and 1.3 seconds (slight departures from the resonance frequency) such instabilities did not errupt until slightly later in the simulation. Lowering the error tolerances on the variable-step Runge-Kutta integrator slightly delayed the onset of instabilities due to the smaller time-steps taken. (Numerical instabilities and methods to suppress or circumvent them have received much attention in the literature on computational free-surface potential flows (see e.g. [20], [25], [34], [35], [46]). The present model incorporates no special measures to delay the onset of instability except for controlling the sizes of the time steps by appropriate selection of the error tolerancing parameters.) At a period of 1.6 seconds, far away from the resonance condition, the calculation was run to 20 seconds with no hint of impending instability.

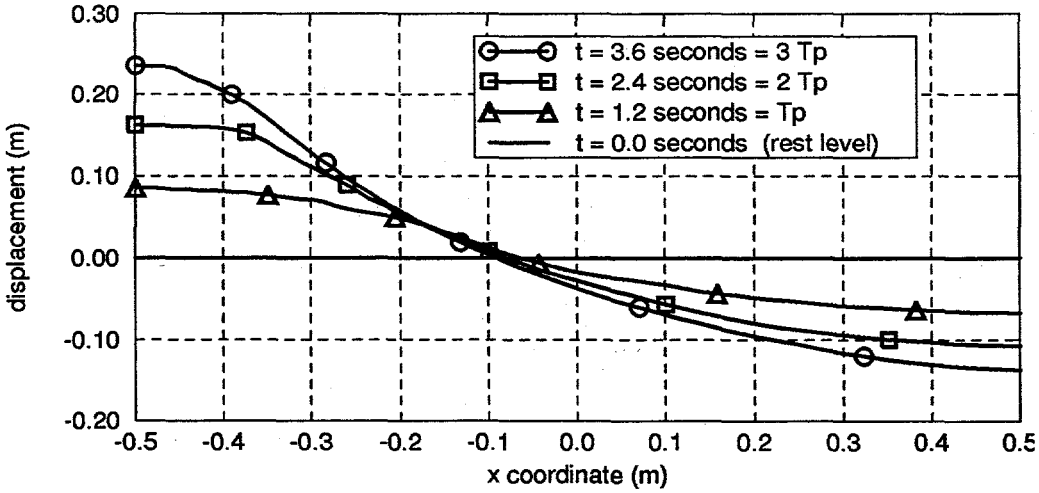


**Figure 7:** Free-surface displacement at multiples of the container oscillation period $T_p$ = 1.2 sec. (near the natural frequency of the liquid).

## VI. Concluding Remarks

The numerical model presented here appears to be more general and qualitatively/quantitatively correct than previously published models for simulating the unsteady nonlinear behavior of an incompressible Rayleigh-damped irrotational liquid within a container subjected to forced horizontal oscillation.

## References


[1] Lamb, H., *Hydrodynamics*, 6th. ed., Dover Publications, New York, 1945.

[2] Currie, I.G., *Fundamental Mechanics of Fluids*, McGraw-Hill Book Co., 1974.

[3] Abramson, H.N., editor, *The Dynamic Behavior of Liquids in Moving Containers*, NASA Sp-106, Washington, 1966.

[4] Abramson, H.N., "Dynamic Behavior of Liquid in Moving Container," Applied Mechanics Reviews (July 1963), vol. 16, no. 7, pp. 501-506.

[5] Fox, D.W., and Kuttler, J.R., "Sloshing frequencies," J. Appl. Mathematics and Phys. (ZAMP), vol. 34, Sept. 1983, pp. 668-696.

[6] Moiseev, N.N., "Introduction to the Theory of Oscillations of Liquid-Containing Bodies," *Advances in Applied Mechanics*, H.L. Dryden and Th. von Karman, eds., vol. 8, Academic Press, 1964, pp. 233-289.

[7] Moiseev, N.N., and Petrov, A. A., "The Calculation of Free Oscillations of a Liquid in a Motionless Container," *Advances in Applied Mechanics*, (1966) vol. 9, pp. 91-154.

[8] Ikegawa, M., "Finite element analysis of fluid motion in a container," in *Finite Element Methods in Flow Problems*, eds. J.T. Oden, O.C. Zienkiewicz, R.H. Gallagher, and C. Taylor, UAH Press, Huntsville, 1974, pp. 737-738

[9] Washizu, K., Nakayama, T., and Ikegawa, M., "Application of the finite element method to some free surface fluid problems," in *Finite Elements in Water Resources*, eds. W.G. Gray, G.F. Pinder, and C.A. Brebbia, Pentech Press, London, 1978, pp. 4.247-4.266.

[10] Aslam, Mohammad, "Finite element analysis of earthquake-induced sloshing in axisymmetric tanks," Int. J. for Num. Mthds. in Engr. (1981), vol. 17, pp. 159-170.

[11] Wellford, L.C., and Ganaba, T.H., "A finite element method with a hybrid Lagrange line for fluid mechanics problems involving large free surface motion," Int. J. for Num. Mthds. in Engr. (1981), vol. 17, pp. 1201-1231.

[12] Salmon, J.R., Liu, P.L-F, and Liggett, J.A., "Integral equation method for linear water waves," J. Hydraulics. Div., ASCE, vol. 106, Dec. 1980, (HY12), pp. 1995-2010.

[13] Nakayama, T., and Washizu, K., "The boundary element method applied to the analysis of two-dimensional nonlinear sloshing problems," Int. J. for Num. Mthds. in Engr. (1981), vol. 17, pp. 1631-1646.

[14] Medina, D.E., Liggett, J.A., Birchwood, R.A., and Torrance, K.E., "A consistent boundary element method for free surface hydrodymanic calculations," Int. J. for Num. Mthds. in Engr. (1991), vol. 12, pp. 835-857.

[15] Faltinsen, O.M., "A numerical nonlinear method of sloshing in tanks with two-dimensional flow," J. Ship Research (Sept. 1978), vol. 22, no. 3, pp. 193-202.

[16] Pauwelussen, "Horizontal nonlinear sloshing using boundary elements," Bounary Elements IX, vol. 3, C.A. Brebbia and W. Wendland eds., Springer-Verlag and Computational Mechanics Publications, 1987, pp. 167-185.

[17] Kim, S.K., Liu, P.L-F., and Liggett, J.A., "Boundary integral equation solutions

for solitary wave generation, propagation, and run-up," Coastal Engineering (1983), vol. 7, pp. 299-317.

[18] Faltinsen, O.M., "Numerical solutions of transient nonlinear free-surface motion outside or inside moving bodies," *Proceedings of the Second International Conference on Numerical Ship Hydrodynamics,* University of California at Berkeley, September 1977, pp. 347-357.

[19] Grilli, S.T., Skourup, J., and Svendsen, I.A., "An efficient boundary element method for nonlinear water waves," Engr. Analysis with Boundary Elements (1989), vol. 6, no. 2, pp. 97-107.

[20] Dommermuth, D.G., and Yue, D.K., "Numerical simulations of nonlinear axisymmetric flows with a free surface," J. Fluid Mech. (1987), vol. 178, pp. 195-219.

[21] Vinje, T., and Brebig, P., "Numerical calculations of forces from breaking waves," in the proceedings *International Symposium on Hydrodynamics in Ocean Engineering*, Norwegian Institute of Technology, 1981, pp. 547-565.

[22] Nakayama, T., "A computational method for simulating transient motions of an incompressible inviscid fluid with a free surface," Int. J. for Num. Mthds. in Engr. (1990), vol. 10, pp. 683-695.

[23] Case, K.M., and Parkinson, W.C., "Damping of surface waves in an incompressible liquid," J. Fluid Mechanics (1957), vol. 2, part 2, pp. 172-184.

[24] Bird, R.B., Stewart, W.E., and Lightfoot, E.N., *Transport Phenomena*, John Wiley & Sons, 1960.

[25] Longuet-Higgins, M.S., and Cokelet, E.D., "The deformation of steep surface waves on water: I. A numerical method of computation," Proc. R. Soc. Lond., Ser. A (1976), vol. 350, pp. 1-26.

[26] Gear, C.W., *Numerical Initial Value Problems in Ordinary Differential Equations*, Prentice-Hall, Englewood Cliffs, N.J., 1971.

[27] Shampine, L.F., and Watts, H.A., "DEPAC--Design of a User Oriented Package of ODE Solvers," Sandia National Labs (Albuquerque, New Mexico, 87185) report SAND79-2374, printed September 1980.

[28] Haskell, K.H., Vandevender, W.H., and Walton, E.L., "The SLATEC Common Mathematical Subprogram Library: SNLA Implementation," Sandia National Labs (Albuquerque, New Mexico, 87185) report SAND80-2792.

[29] Dold, J.W., and Peregrine, D.H., "Steep unsteady water waves: An efficient computational scheme," in *Proc. 19th Int'l. Conf. on Coastal Engr.*, 1984, pp. 955-967.

[30] Nakayama, T., "Boundary element analysis of nonlinear water wave problems," Int. J. for Num. Mthds. in Engr. (1983), vol. 19, pp. 953-970.

[31] Grilli, S., "Application of the Boundary Element Method to some elliptic fluid mechanics problems," in *Proceedings of the First Intl. Conf. on Computer Methods and Water Resources*, Rabat, Morocco, 1988, vol. 4 (eds. D. Ouazar and C.A. Brebbia), Computational Mechanics Publications, Springer-Verlag, Berlin, pp. 97-113.

[32] Yeung, R.W., "Numerical Methods in Free-Surface Flows," *Ann. Rev. Fluid Mech.*, vol. 14, Annual Reviews Inc., 1982, pp. 395-442.

[33] Brebbia, C.A., Telles, J.C.F., and Wrobel, L.C., *Boundary Element Techniques*, Springer-Verlag, Berlin, 1984.

[34] Dold, J.W., "An efficient surface-integral algorithm applied to unsteady gravity waves," J. Comp. Phys. (1992), vol. 103, pp. 90-115.

[35] Pelekasis, N.A., Tsamopoulos, J.A., and Manolis, G.D, "A hybrid finite-boundary element method for inviscid flows with free surfaces," J. Comp. Phys. (1992, August), vol. 101, pp. 231-251.

[36] Banerjee, G.R., and Butterfield, R., *Boundary Element Method in Engineering Science*, McGraw-Hill, U.K., 1981.

[37] Liggett, J.A., and Salmon, J.R., "Cubic spline boundary elements," Int. J. for Num. Mthds. in Engr. (1981), vol. 17, pp. 543-556.

[38] Cabral, J.J.S.P., and Wrobel, L.C., "Application of B-spline boundary elements to groundwater flow problems," in *Proceedings of Computational Modeling of Free and Moving Boundary Problems, Vol. 1 Fluid Flow*, First Int'l. Conf., July 2-4, 1991, Southampton, U.K., eds. L.C. Wrobel and C.A. Brebbia, copublished by Computational Mechanics Publications and Walter de Gruyter, 1991, pp. 20-36.

[39] Ortiz, J.C., and Douglass, S.L., "Overhauser boundary elements solution for periodic water waves in the physical plane," Engr. Anal. with Boundary Elements (1993), vol. 11, pp. 47-54.

[40] Grilli, S.T., and Svendsen, I.A., "Corner problems and global accuracy in the boundary element solution of nonlinear wave flows," Engr. Analysis with Boundary Elements (1990), Vol. 7, No. 4, pp. 178-195.

[41] Ingber, M.S., and Schreyer, H.L., "Construction of stiffness matrices to maintain the convergence rate of distorted finite elements," Int. J. for Num. Mthds. in Engr. (1993), vol. 36, pp. 1927-1944.

[42] Mitra, A.K., and Ingber, M.S., "A multiple-node method to resove the difficulties in the boundary integral equation method caused by corners and discontinuous boundary conditions," Int'l. J. for Num. Mthds. in Engr. (1993), vol. 36, pp. 1735-1746.

[43] Muci-Kuchler, K.H., and Rudolphi, T.J., "Application of tangent derivative boundary integral equations to the solution of elastostatics problems," *Boundary Element Technology VII*, eds. C.A. Brebbia and M.S. Ingber, proceedings of BETECH '92, U. of New Mexico, USA, Computational Mechanics Publications copublished with Elsevier Applieed Science, 1992, pp. 757-774.

[44] Liu, P.L-F., and Liggett, J.A., "Boundary element formulations and solutions for some nonlinear water wave problems," Chapter 7 of *Developments in Boundary Element Methods - 3*, P.K. Banerjee and S. Murkerjee, eds., Elsevier Applied Science Publishers, 1984, pp. 171-190.

[45] Cointe, R., "Remarks on the numerical treatment of the intersection point between a rigid body and a free surface," in *Proc. 3rd Int'l. Workshop on Water Waves and Floating Bodies*, Woods Hole, MA, USA, 1988.

[46] Baker, G.R., Meiron, D.I., and Orszag, S.A., "Generalized vortex methods for free-surface flow problems," J. Fluid Mech. (1982), vol. 123, pp. 477-501.